

## Coulomb effects on the electron scattering radiation tail

Indu Talwar, L. E. Wright, D. S. Onley, and C. W. Soto Vargas\*

*Department of Physics, Ohio University, Athens, Ohio 45701*

(Received 14 July 1986)

We carry out a distorted wave calculation of the radiation tail accompanying relativistic elastic electron scattering from the atomic nucleus using recently developed techniques for evaluating the radial matrix elements entering the calculation. The difficulty of calculating the high multipole components of the bremsstrahlung cross section is avoided by introducing a distortion factor that can be evaluated within the required accuracy with about 20 photon multipoles. The calculation still requires extensive computational time, so we compare our distorted wave results to an *ad hoc* technique of including distortion in the Bethe-Heitler result that is widely used. Surprisingly, we find that the *ad hoc* technique is very good for energy losses less than about 70% of the incident electron energy.

### I. INTRODUCTION

A problem of long standing in the analysis of inelastic electron scattering from medium and heavy nuclei has been the evaluation of the radiation tail which accompanies elastic electron scattering. In single arm electron scattering experiments, only the scattered electron is detected at some scattering angle  $\theta_e$  and some energy loss  $\Delta E$ . However, electrons which scatter elastically from the nucleus and also emit a real photon of energy  $\omega = \Delta E$  (bremsstrahlung with neglect of the recoil kinetic energy of the nucleus) cannot be distinguished from electrons which transfer energy  $\omega$  to the nucleus. Although the bremsstrahlung accompanying an electron scattered through a large angle  $\theta_e$  is a very small fraction of the total bremsstrahlung, the elastic scattering cross section is so much larger than inelastic scattering cross sections that, apart from special cases, the radiation tail is comparable to or larger than inelastic scattering cross sections.

The radiation tail along with a number of radiative effects accompanying electron scattering from the atomic nucleus can be calculated in a rather straightforward manner in the plane wave approximation where the incoming and outgoing electron wave functions are taken to be Dirac plane waves. In the plane wave approximation, the radiation tail accompanying elastic electron scattering is a two photon process and can be evaluated by integrating the Bethe-Heitler formula<sup>1</sup> over emitted photon angles. The finite size of the nucleus is included by introducing a charge form factor at the nuclear vertex. The details of this integration are given in Maximon and Isabelle<sup>2</sup> and in the work of Mo and Tsai.<sup>3,4</sup> The latter authors also discuss in some detail and give explicit prescriptions for calculating other radiative effects such as atomic screening, Schwinger corrections, and the radiation tail accompanying inelastic peaks. Their work seems to be used by almost all electrons scattering experimental groups to extract their inelastic electron scattering cross sections arising from nuclear processes. For medium and heavy nuclei ( $Z \geq 20$ ), however, the plane wave results for the radiation tail accompanying elastic scattering should

only be of qualitative assistance in extracting the inelastic cross sections from the measured data, and even the qualitative assistance is not very helpful when the nuclear excited states or the inelastic process under investigation is broad such as in the cases of giant resonances or quasi-elastic scattering.

The correct way of including the Coulomb effects in the radiation tail is well known. One need only do a distorted wave calculation where the large static Coulomb field of the nucleus is included in the Dirac equation for the incoming and outgoing electrons. The emission of a real photon is then treated in Born approximation. That is, one does a distorted wave Born approximation (DWBA) calculation of the radiation tail. However, use of Dirac-Coulomb wave functions seems to require partial wave expansions of the wave functions, and thus a multipole expansion of the photon field in order to evaluate the angular matrix elements. This generates large numbers of radial matrix elements since the partial wave series and multipole sums are slowly converging, and these radial matrix elements are difficult to evaluate. Recent work on the mathematics of the Dirac-Coulomb functions and integrals over them<sup>5-7</sup> has provided the necessary tools for evaluating these radial integrals. The cross section formulas for the DWBA radiation tail along with a brief summary of the techniques for evaluating the radial integrals is given in Sec. II and the Appendix. In Sec. III, a distortion factor which requires a multipole decomposition of the Bethe-Heitler formula is introduced to aid in summing the multipole series.

The difficulty of subtracting the radiation tail accompanying inelastic electron scattering from medium and heavy nuclei has existed for many years, and an *ad hoc* method of including the Coulomb distortion was developed quite early. While the *ad hoc* method of including the effects of Coulomb distortion is intuitively appealing and takes far less computer time than a full DWBA calculation, there does not exist much theoretical justification for the procedure. In Sec. IV, we discuss the *ad hoc* procedure and compare it to our distorted wave results, and examine its use in a recent experiment which

measured the radiation tail.<sup>8</sup> In Sec. V, we summarize our findings and make recommendations on how to best treat the Coulomb effects on the radiation tail accompanying elastic electron scattering.

## II. THE RADIATION TAIL IN DWBA

The Hamiltonian density for electrons in a static electromagnetic field and photons is

$$H = H_{\text{rad}} + H_{\text{DC}} + H_{\text{int}}, \quad (1)$$

where the Hamiltonian for the electromagnetic field in free space in second quantized form can be written as

$$H_{\text{rad}} = \sum_{\mathbf{k}, \lambda} (a_{\mathbf{k}, \lambda}^\dagger a_{\mathbf{k}, \lambda} + \frac{1}{2}). \quad (2)$$

In the radiation gauge this corresponds to the potentials

$$\begin{aligned} \Phi(\mathbf{r}, t) &= 0, \\ \mathbf{A}(\mathbf{r}, t) &= \sum_{\mathbf{k}, \lambda} \left[ \frac{2\pi}{\omega_{\mathbf{k}}} \right]^{1/2} [a_{\mathbf{k}, \lambda} \mathbf{u}_{\mathbf{k}, \lambda}(\mathbf{r}) e^{-i\omega_{\mathbf{k}} t} + a_{\mathbf{k}, \lambda}^\dagger \mathbf{u}_{\mathbf{k}, \lambda}^* e^{i\omega_{\mathbf{k}} t}], \end{aligned} \quad (3)$$

where

$$\mathbf{u}_{\mathbf{k}, \lambda} = \left[ \frac{1}{V} \right]^{1/2} \hat{\mathbf{e}}_\lambda e^{i\mathbf{k} \cdot \mathbf{r}}$$

and  $\lambda$  denotes the polarization state of photons propagating with momentum  $\mathbf{k}$  and  $V$  is the normalization volume. The spherically symmetric static Coulomb potential of the nucleus,  $V(r)$ , is included in the Dirac-Coulomb Hamiltonian

$$H_{\text{DC}} = -i\boldsymbol{\alpha} \cdot \nabla + V(r) + m\beta, \quad (4)$$

where  $\boldsymbol{\alpha}$  and  $\beta$  are the standard Dirac matrices. The Dirac-Coulomb wave functions are solutions to the equation

$$H_{\text{DC}} \psi(\mathbf{r}) = E \psi(\mathbf{r}) \quad (5)$$

and their expansions into partial waves for spin projection  $m_i$  of the electron is

$$\begin{aligned} \psi^{m_i}(\mathbf{r}) &= 4\pi \left[ \frac{E+m}{2EV} \right]^{1/2} \sum_{\kappa, \mu} e^{i\delta_{\kappa i}} C_{\mu - m_i, m_i}^{l, 1/2, j} \\ &\quad \times Y_l^{\mu - m_i}(\hat{\mathbf{p}}) \psi_\kappa^\mu(\mathbf{r}), \end{aligned} \quad (6)$$

where the spinor is

$$\psi_\kappa^\mu(\mathbf{r}) = \begin{bmatrix} g_\kappa(r) & \chi_\kappa^\mu(\hat{\mathbf{r}}) \\ if_\kappa(r) & \chi_{-\kappa}^\mu(\hat{\mathbf{r}}) \end{bmatrix} \quad (7)$$

and  $\kappa$  is the Dirac quantum number which determines  $l$  and  $j$  in the usual way.

The interaction Hamiltonian between the electromagnetic field and the electron is

$$H_{\text{int}} = \rho \phi(\mathbf{r}, t) - \mathbf{J} \cdot \mathbf{A}(\mathbf{r}, t), \quad (8)$$

where the current operator  $\mathbf{J} = e\boldsymbol{\alpha}$ . By using eigenstates of  $H_{\text{rad}} + H_{\text{DC}}$  as basis functions and treating  $H_{\text{int}}$  by first order perturbation theory (i.e., one photon exchange), the scattering amplitude for an electron with energy  $E_1$  and spin  $m_1$  to emit a photon with energy (momentum)  $\omega(\mathbf{k})$  and polarization  $\lambda$  leaving an electron with energy  $E_2$  and spin  $m_2$  is given by

$$a_{f,i} = 2\pi i \delta(E_2 + \omega - E_1) u_{f,i}, \quad (9)$$

where

$$u_{f,i} = e \left[ \frac{2\pi}{\omega V} \right]^{1/2} \int \psi_2^{m_2 \dagger} \boldsymbol{\alpha} \cdot \hat{\mathbf{e}}_\lambda^* e^{-i\mathbf{k} \cdot \mathbf{r}} \psi_1^{m_1} d^3r. \quad (10)$$

The triple differential cross section for bremsstrahlung is given in terms of the scattering amplitude by

$$\frac{d^3\sigma}{d\omega d\Omega_e d\Omega_\gamma} = \frac{1}{2} \sum_{\lambda, m_1, m_2} \frac{2\pi}{I_e} |u_{f,i}|^2 \frac{d^2n_e}{dE_2 d\Omega_e} \frac{d^2n_\gamma}{d\omega d\Omega_\gamma}, \quad (11)$$

where the initial electron flux  $I_e = p_1/E_1 V$  and the density of state factors are

$$\frac{d^2n_e}{dE_2 d\Omega_e} = \frac{V p_2 E_2}{(2\pi)^3}, \quad \frac{d^2n_\gamma}{d\omega d\Omega_\gamma} = \frac{V \omega^2}{(2\pi)^3}. \quad (12)$$

In order to perform the angular integral in Eq. (10) we expand the photon field into multipoles by writing

$$\begin{aligned} \mathbf{A}_\lambda(\mathbf{r}, t) &= \hat{\mathbf{e}}_\lambda e^{i\mathbf{k} \cdot \mathbf{r}} \\ &= \lambda (2\pi)^{1/2} \sum_{LM} \hat{L}^L D_{M\lambda}^L(\hat{\mathbf{k}}) \\ &\quad \times [\mathbf{A}_{LM}^{(m)}(\mathbf{r}) + i\lambda \mathbf{A}_{LM}^{(e)}(\mathbf{r})], \end{aligned} \quad (13)$$

where  $\hat{\mathbf{e}}_\lambda$  is in a spherical basis,  $\hat{L} = (2L+1)^{1/2}$ , and  $D_{M,\lambda}^L(\hat{\mathbf{k}})$  are the rotation matrices which describe the angular distribution of photons. The magnetic and electric multipole fields are given by

$$\mathbf{A}_{LM}^{(m)}(\mathbf{r}) = j_l(kr) \mathbf{Y}_{L,L}^M(\hat{\mathbf{r}}), \quad (14)$$

$$\begin{aligned} \mathbf{A}_{LM}^{(e)}(\mathbf{r}) &= \left[ \frac{L+1}{2L+1} \right]^{1/2} j_{L-1}(kr) \mathbf{Y}_{L,L-1}^M(\hat{\mathbf{r}}) \\ &\quad - \left[ \frac{L}{2L+1} \right]^{1/2} j_{L+1}(kr) \mathbf{Y}_{L,L+1}^M(\hat{\mathbf{r}}). \end{aligned} \quad (15)$$

These expansions permit us to carry out the angular integral in Eq. (10), but for subsequent calculation of the remaining radial integral it is convenient to switch to the least singular gauge. That is, we choose

$$\mathbf{A}'_\lambda(\mathbf{r}) = \mathbf{A}_\lambda(\mathbf{r}) + \nabla S_\lambda(\mathbf{r}) \quad (16)$$

and

$$\phi'_\lambda(\mathbf{r}) = i\omega S_\lambda(\mathbf{r}), \quad (17)$$

where the time independent part of the gauge function is

$$S_{\lambda}(\mathbf{r}) = \frac{(2\pi)^{1/2}}{\omega} \sum_{L,M} i^{L+1} \hat{L} \left[ \frac{L}{L+1} \right]^{1/2} D_{M,\lambda}^L(\hat{\mathbf{k}}) \times j_L(\omega r) Y_L^M(\hat{\mathbf{r}}). \quad (18)$$

Since we now have a scalar potential we also need the charge operator for the electrons in Eq. (8).

Substituting the partial wave expansion of Eq. (6) for the initial and final electron states and the photon multipole expansion in the least singular gauge in Eq. (10) and carrying out the angular integral and the requisite Dirac algebra we obtain

$$u_{f,i} = \lambda 4\pi^2 \left[ \frac{(E_1+m)(E_2+m)}{E_1 E_2 \omega V^3} \right]^{1/2} \sum_{\kappa_1, \kappa_2, L, M} (-1)^M e^{i(\delta_{\kappa_1} + \delta_{\kappa_2})} i^{l_1 - l_2 - L - 1} (-1)^{j_1 + 1/2} \times D_{-M,\lambda}^{L*}(\hat{\mathbf{k}}) \hat{l}_1 \hat{L} \hat{j}_1 C_{0m_1 m_1}^{l_1 1/2 j_1} C_{m_1 + M - m_2 m_2 m_1 + M}^{l_2 1/2 j_2} \times C_{-1/2 1/2 0}^{j_1 j_2 L} C_{m_1 M m_1 + M}^{j_1 L j_2} R(\kappa_1, \kappa_2, L, \lambda) Y_{l_2}^{m_1 - m_2 + M}(\hat{\mathbf{p}}_2), \quad (19)$$

where the initial electron momentum  $\mathbf{p}_1$  has been chosen to define the  $z$  axis. The radial integrals in Eq. (19) are given by

$$R(\kappa_1, \kappa_2, L, \lambda) = \left[ \frac{1 + (-1)^{l_1 + l_2 + L}}{2} \right] I^{(m)} + i\lambda \left[ \frac{1 + (-1)^{l_1 + l_2 + L}}{2} \right] I^{(e)}, \quad (20)$$

where  $\bar{l} = l(-\kappa)$  and the magnetic and electric radial integrals in the least singular gauge are given by

$$I^{(m)} = \frac{\kappa_1 + \kappa_2}{[L(L+1)]^{1/2}} \int_0^\infty j_L(\omega r) (f_{\kappa_1} g_{\kappa_2} + g_{\kappa_1} f_{\kappa_2}) r^2 dr \quad (21)$$

and

$$I^{(e)} = \left[ \frac{L}{L+1} \right]^{1/2} \int_0^\infty \left[ j_{L-1}(\omega r) \left( f_{\kappa_1} g_{\kappa_2} - g_{\kappa_1} f_{\kappa_2} \right) + \frac{\kappa_1 - \kappa_2}{L} (f_{\kappa_1} g_{\kappa_2} + g_{\kappa_1} f_{\kappa_2}) \right] + j_L(\omega r) (f_{\kappa_1} f_{\kappa_2} + g_{\kappa_1} g_{\kappa_2}) r^2 dr. \quad (22)$$

Additional details of this derivation may be found in Refs. 5, and 9–11.

To obtain the DWBA radiation tail, we integrate the triply differential cross section of Eq. (11) over photon angles using the orthogonality properties of the rotation matrices to obtain

$$\frac{d^2\sigma}{d\omega d\Omega_e} = \sum_{L=1}^{\infty} a_L(T_1, \omega, \theta_e; \mathbf{Z}), \quad (23)$$

where the contribution of photons of multipolarity  $L$  for electrons with initial kinetic energy  $T_1$  is given by

$$a_L(T_1, \omega, \theta_e; \mathbf{Z}) = \frac{4\alpha\omega(E_1+m)(E_2+m)p_2}{p_1} \times \sum_{M, m_2} \left| \sum_{\kappa_1, \kappa_2} e^{i(\delta_{\kappa_1} + \delta_{\kappa_2})} i^{l_1 - l_2} (-1)^{j_1 + 1/2} \hat{l}_1 \hat{j}_1 C_{0 1/2 1/2}^{l_1 1/2 j_1} \times C_{1/2 - M - m_2 m_2 1/2 - M}^{l_2 1/2 j_2} C_{-1/2 1/2 0}^{j_1 j_2 L} C_{1/2 - M 1/2 - M}^{j_1 L j_2} R(\kappa_1, \kappa_2, L, \lambda) Y_{l_2}^{1/2 - M - m_2}(\hat{\mathbf{p}}_2) \right|^2 \quad (24)$$

and the sums over initial electron spin and photon polarization have been performed. Note that due to the selection rules implicit in Eq. (20), the electric and magnetic integrals in  $R$  enter incoherently and hence are independent of the photon polarization.

Two difficulties arise in evaluating the cross section given in Eqs. (23) and (24). They are the evaluation of the

radial integrals given in Eqs. (21) and (22) and performing the sum over photon multipoles  $L$ . We will discuss the evaluation of the radial integrals before turning to performing the multipole sum.

The Dirac-Coulomb wave functions in the integrand of Eqs. (21) and (22) satisfy the first order coupled differential equation

$$\begin{aligned} & \frac{d}{dr} \begin{pmatrix} g_\kappa \\ f_\kappa \end{pmatrix} \\ &= \frac{1}{r} \begin{pmatrix} -\kappa-1 & 0 \\ 0 & \kappa-1 \end{pmatrix} \begin{pmatrix} g_\kappa \\ f_\kappa \end{pmatrix} \\ &+ \begin{pmatrix} 0 & +[E+m-V(r)] \\ -[E-m-V(r)] & 0 \end{pmatrix} \begin{pmatrix} g_\kappa \\ f_\kappa \end{pmatrix}, \end{aligned} \quad (25)$$

where  $V(r)$  is the static Coulomb field of the nucleus. For values of  $r$  inside the nuclear interior, Eq. (25) cannot be solved analytically for a general charge distribution and we generate the electron wave functions by numerical integration. However, for values of the radial coordinate outside some cutoff radius  $R$ , the potential  $V(r)$  reduces to  $-\alpha Z/r$ , and we can rewrite Eq. (25) in the following matrix form:

$$\frac{d}{dr} u^{(S)} = \left[ \frac{A^{(S)}}{r} - B^{(S)} \right] u^{(S)}, \quad (26)$$

where  $u^{(S)}$  and the matrices  $A^{(S)}$  and  $B^{(S)}$  are given by the following:

$$\begin{aligned} u^{(S)} &= \begin{pmatrix} r g_\kappa \\ r f_\kappa \end{pmatrix}, \\ A^{(S)} &= \begin{pmatrix} -\kappa & \alpha Z \\ -\alpha Z & \kappa \end{pmatrix}, \\ B^{(S)} &= \begin{pmatrix} 0 & -(E+m) \\ E-m & 0 \end{pmatrix}. \end{aligned} \quad (27)$$

The Dirac-Coulomb wave functions have been extensively investigated and we only quote the solutions in order to clarify the notation. The regular Dirac-Coulomb functions can be expressed in terms of the Whittaker function by

$$\begin{aligned} \begin{pmatrix} r g_\kappa^R \\ r f_\kappa^R \end{pmatrix} &= \begin{pmatrix} 1 \\ -\left[ \frac{E-m}{E+m} \right]^{1/2} \end{pmatrix} \frac{(2pr e^{-\eta\pi})^{1/2} |\Gamma(\gamma+i\eta)|}{p\Gamma(2\gamma+1)} \\ &\times \begin{pmatrix} R_e \\ I_m \end{pmatrix} (\gamma+i\eta) e^{-i(\gamma+1/2)\pi/2} \\ &\times e^{i\eta\kappa} M_{-i\eta, \gamma-1/2}(2ipr), \end{aligned} \quad (28)$$

where the parameters are  $\gamma = (\kappa^2 - \alpha^2 Z^2)^{1/2}$ ,  $\eta = \alpha Z E / p$ ,  $p = (E^2 - m^2)^{1/2}$ , and the phase  $\eta_\kappa$  is given by

$$\eta_\kappa(\gamma) = \frac{-\pi}{2} \left[ \frac{1+S_\gamma S_\kappa}{2} \right] - \frac{1}{2} \arctan \left[ \frac{\beta\gamma + \kappa\eta}{\kappa\gamma - \eta\beta} \right] \quad (29)$$

with  $S_\gamma = \gamma / |\gamma|$  and  $S_\kappa = \kappa / |\kappa|$ . We choose to define our irregular solutions, labeled by  $I$ , such that they are obtained from the regular solutions by adopting the negative sign for  $\gamma$  everywhere in Eqs. (28) and (29). For later use,

note that when  $Z \rightarrow 0$ ,  $m \rightarrow 0$ , and  $p \rightarrow \omega$ , the solutions in Eq. (28) reduce to

$$u_L = \begin{pmatrix} r j_L(\omega r) \\ r j_{L-1}(\omega r) \end{pmatrix} \quad (30)$$

for  $L = \kappa > 0$ , and furthermore  $u_L$  satisfies Eq. (26) with the following  $A$  and  $B$  matrices:

$$A = \begin{pmatrix} -L & 0 \\ 0 & L \end{pmatrix}, \quad B = \begin{pmatrix} 0 & -\omega \\ \omega & 0 \end{pmatrix}. \quad (31)$$

The wave functions in the external region are a linear combination of the regular and irregular Dirac-Coulomb solutions given above,

$$\begin{pmatrix} g_\kappa \\ f_\kappa \end{pmatrix} = \begin{pmatrix} g_\kappa^R & g_\kappa^I \\ f_\kappa^R & f_\kappa^I \end{pmatrix} \begin{pmatrix} A_\kappa \\ B_\kappa \end{pmatrix} \quad \text{for } r \geq R, \quad (32)$$

where the constants  $A_\kappa$  and  $B_\kappa$  can be extracted at any point  $r$  outside the nuclear charge distribution. They are given by

$$A_\kappa = \frac{f_\kappa^I g_\kappa^R - f_\kappa^R g_\kappa^I}{f_\kappa^I g_\kappa^R - g_\kappa^I f_\kappa^R}, \quad B_\kappa = \frac{f_\kappa^I g_\kappa^R - g_\kappa^I f_\kappa^R}{f_\kappa^I g_\kappa^R - g_\kappa^I f_\kappa^R}. \quad (33)$$

Expressing the scattering phase shift  $\delta_\kappa$  needed in Eq. (24) in terms of a point phase  $\Delta_\kappa$  and a phase due to the finite nuclear size  $\bar{\delta}_\kappa$ , by writing  $\delta_\kappa = \Delta_\kappa + \bar{\delta}_\kappa - (l+1)\pi/2$ , we find that

$$\tan \bar{\delta}_\kappa = \frac{\sin \bar{\theta}_\kappa}{A_\kappa / B_\kappa + \cos \bar{\theta}_\kappa}, \quad (34)$$

where we have introduced  $\bar{\theta}_\kappa = \Delta_\kappa^I - \Delta_\kappa^R$  which is given explicitly by

$$\begin{aligned} \bar{\theta}_\kappa &= -\pi(\kappa - \gamma) - \arctan(\tan \pi(\kappa - \gamma) \coth \pi\eta) \\ &+ \frac{\pi}{2} + \frac{\pi}{2} S_\kappa. \end{aligned} \quad (35)$$

The regular point phase shift  $\Delta_\kappa^R$  is defined as

$$\Delta_\kappa^R = \eta_\kappa(\gamma) - \frac{\pi\gamma}{2} - \arg \Gamma(\gamma + i\eta) + \eta \ln 2pr \quad (36)$$

and the irregular point phase  $\Delta_\kappa^I$  is obtained by changing the sign of  $\gamma$  everywhere in Eq. (36).

The above results imply that for nonpenetrating orbits and for the external region of penetrating orbits the integrands of the required radial integrals are simply integrals over Whittaker functions and, therefore, can be integrated analytically. The evaluation of such integrals by means of matrix series and the analytic continuation of the resulting generalized hypergeometric functions has been investigated extensively.<sup>5,12,13</sup> The general strategy is to make use of the fact that the Dirac-Coulomb wave functions satisfy a first order matrix differential equation whose structure is similar to the scalar first order differential equation satisfied by the integrand of the  $\Gamma$  function. This permits the definition of a matrix  $\Gamma$  function<sup>5,12</sup> with many recursive and differential properties<sup>5,11</sup> which allow new analytic continuation techniques to be applied to the resulting matrix series<sup>5</sup> and the evaluation

of integrals. It is useful to note that the Dirac-Coulomb functions in the standard representation are real, and thus the integrals over spherical Bessel functions in Eqs. (21) and (22) can be obtained by taking the real part of the integrals over spherical Hankel functions which, apart from an exponential, have a finite series expansion in inverse powers of  $r$ . In the Appendix we give the necessary details and the explicit formulas for the radial integrals that occur in bremsstrahlung.

The expression for  $a_L$  given in Eq. (24) contains a coherent sum over  $\kappa_2$ , the Dirac quantum number of the outgoing electron, and  $\kappa_1$  which ranges in magnitude from  $|\kappa_2| - L$  to  $|\kappa_2| + L$  for fixed  $L$ . The series reduction technique of Yennie and Ravenhall<sup>14</sup> works very well in speeding the convergence of this coherent sum over spherical harmonics for electron scattering angles away from  $0^\circ$ . We find that the maximum value of  $\kappa_2$  needed is the greater of  $E_1/5$  (MeV) or  $2L$ , while the number of  $\kappa_1$  terms for a given  $\kappa_2$  is proportional to  $(2L + 1)$ . Thus, for large  $L$  values the number of radial integrals is proportional to  $L^2$  and requires proportionately more computer time. To reduce the time spent in calculating radial integrals we make use of a recursion relation on  $L$  (Ref. 10) given in the Appendix.

The radial integrals with either  $|\kappa_1|$  or  $|\kappa_2|$  less than or equal to some  $\kappa_{\text{mod}}$  contain electron waves which penetrate the nucleus appreciably and require numerical integration over the nuclear interior in addition to asymptotic expansions for the integral from  $R$  to infinity as discussed in the Appendix. When  $|\kappa_1|$  and  $|\kappa_2|$  are both greater than  $\kappa_{\text{mod}}$ , we use the point radial integrals. For incident electron energy of 100 MeV,  $\kappa_{\text{mod}} = 7$  is sufficient.

### III. DISTORTION FACTORS

Using the radial integrals given in the Appendix along with the series reduction technique of Yennie and Ravenhall, we can calculate  $a_L(T_1, \omega, \theta_e; Z)$  for any electron scattering angle  $\theta_e \geq 20^\circ$  and all values of  $T_1$ ,  $\omega$ , and  $Z$ . However, for large  $L$  values, the number of radial integrals increases rapidly and the incoherent  $L$  sum in Eq. (23) is usually slowly convergent. Without unlimited computer time, this series cannot be summed directly. In a previous investigation of virtual photon spectra,<sup>11</sup> we found that comparing distorted wave contributions to plane wave contributions (designated by  $Z = 0$ ) was useful

in summing slowly converging series. While the radiation tail is quite different from the virtual photon spectrum, we consider the use of some sort of distortion factor.

Defining a multipole distortion factor

$$d_L(T_1, \omega, \theta_e; Z) = \frac{a_L(T_1, \omega, \theta_e; Z)}{a_L(T_1, \omega, \theta_e; 0)} \quad (37)$$

and assuming that, for some  $L \geq L_{\text{max}}$ ,  $d_L$  approaches a constant, the distorted wave radiation tail can be written as

$$\frac{d^2\sigma}{d\omega d\theta_e} = \sum_{L=1}^{L_{\text{max}}} [a_L(Z) - d_{L_{\text{max}}} a_L(0)] + d_{L_{\text{max}}} \left[ \frac{d^2\sigma}{d\omega d\theta_e} \right]^{\text{PW}}, \quad (38)$$

where only the  $Z$  dependence is shown in  $a_L$  and PW designates the plane wave. We also consider a distortion factor defined by

$$D_{L_{\text{max}}}(T_1, \omega, \theta_e; Z) = \frac{\sum_{L=1}^{L_{\text{max}}} a_L(T_1, \omega, \theta_e; Z)}{\sum_{L=1}^{L_{\text{max}}} a_L(T_1, \omega, \theta_e; 0)}, \quad (39)$$

where again  $Z = 0$  corresponds to plane waves. While we could obtain the plane wave result by running our general code for very small  $Z$ , it is more accurate and considerably faster to carry out a multipole decomposition of the Bethe-Heitler result which we give in the Appendix. To our knowledge this result has not been given before. If for some finite  $L_{\text{max}}$ ,  $D_L$  approaches a constant, say  $D^{\text{DW}}$ , the distorted wave cross section is given by

$$\frac{d^2\sigma}{d\omega d\Omega_e} = D^{\text{DW}} \left[ \frac{d^2\sigma}{d\omega d\Omega_e} \right]^{\text{PW}}. \quad (40)$$

The value of the plane wave result is given by Mo and Tsai<sup>3,4</sup> and by Maximon and Isabelle.<sup>2</sup> In Maximon and Isabelle's notation

$$\left[ \frac{d^2\sigma}{d\omega d\Omega_e} \right]^{\text{PW}} = \frac{Z^2 \alpha^3}{2\pi} \frac{p_2}{p_1} \int_{q_m^2}^{q_M^2} \frac{d(q^2)}{q^4} F^2(q) \left[ -\frac{2}{(2\lambda + k^2)^{1/2}} - \left( \frac{1}{D_1^{1/2}} - \frac{1}{D_2^{1/2}} \right) \frac{q^4 + 4\lambda^2 - 4q^2(E_1^2 + E_2^2 - m^2) - 16E_1E_2}{2\lambda - q^2} \right. \\ \left. + \frac{2(4E_2^2 - q^2)}{D_1^{3/2}} [2\lambda(\lambda - kE_2) - (\lambda + kE_1)q^2] \right. \\ \left. - \frac{2(4E_1^2 - q^2)}{D_2^{3/2}} [2\lambda(\lambda + kE_1) - (\lambda - kE_2)q^2] \right], \quad (41)$$

where

$$\begin{aligned}
 \lambda &= E_1 E_2 - p_1 p_2 \cos \theta_e - m^2, \\
 D_1 &= [p_1(q^2 - q_2^2) + 2p_2 \lambda_0 \cos \theta_e]^2 + 4k^2 p_2^2 \sin^2 \theta_e, \\
 D_2 &= [p_2(q^2 - q_1^2) + 2p_1 \lambda_0 \cos \theta_e]^2 + 4k^2 p_1^2 \sin^2 \theta_e, \\
 \lambda_0 &= E_1 E_2 - p_1 p_2 - m^2, \\
 q_m &= |\mathbf{p}_1 - \mathbf{p}_2| - k = (2\lambda + k^2)^{1/2} - k, \\
 q_M &= |\mathbf{p}_1 - \mathbf{p}_2| + k = (2\lambda + k^2)^{1/2} + k, \\
 q_2 &= 2p_2 \sin \frac{\theta_e}{2}, \\
 q_1 &= 2p_1 \sin \frac{\theta_e}{2},
 \end{aligned} \tag{42}$$

and  $F(q)$  is the plane wave form factor of the spherically symmetric ground state charge distribution and is given by

$$F(q) = \int \rho(r) j_0(qr) r^2 dr. \tag{43}$$

The form factor is normalized such that  $F(0) = 1$ .

We investigate the behavior of these two distortion factors for 100 MeV electrons scattering from uranium. We take the ground state charge distribution to be given by a two parameter Fermi distribution

$$\rho(r) = \rho_0 / \{1 + \exp[(r - c)/z_1]\}, \tag{44}$$

where the radius and skin-thickness parameters are  $c = 6.84$  fm and  $z_1 = 0.545$  fm. In Fig. 1 we show the ratios  $d_L$  as a function of  $L$  for an energy loss  $\omega = 20$  MeV and electron scattering angles of  $40^\circ$ ,  $100^\circ$ , and  $145^\circ$ . Clearly  $d_L$  is either approximately constant or oscillates about an approximately constant value for large  $L$  values. In Fig. 2 we show the ratio  $D_L$  for the same cases which

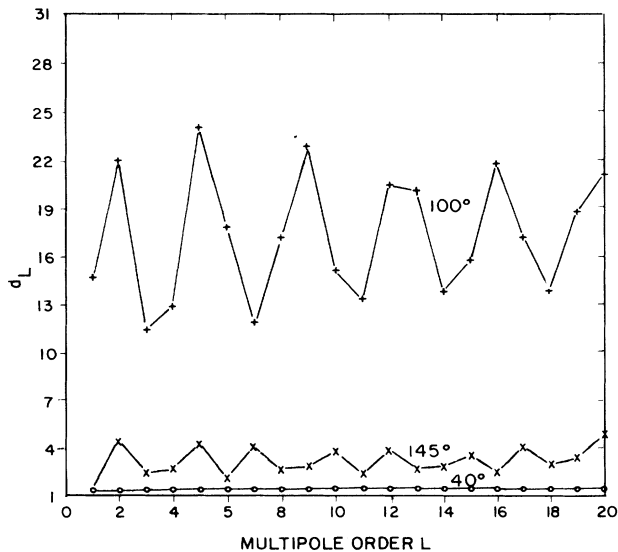


FIG. 1. Distortion factor  $d_L$  as a function of photon multipole  $L$  for  $Z=92$ , incident electron kinetic energy  $T_1=100$  MeV, photon energy  $\omega=20$  MeV, and scattering angles of  $40^\circ$ ,  $100^\circ$ , and  $145^\circ$ .

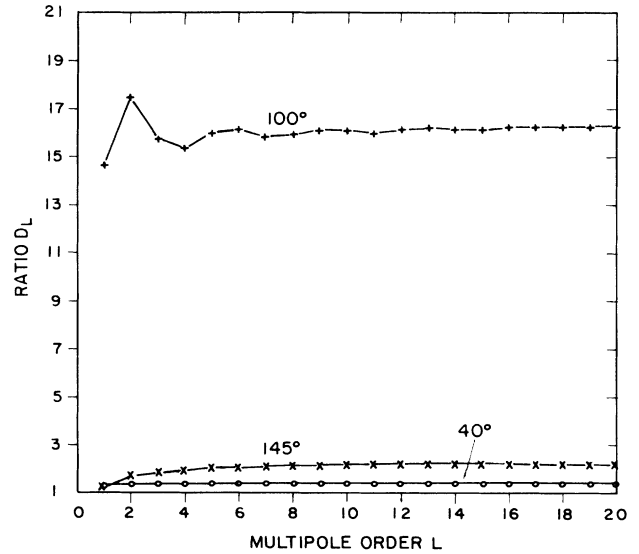


FIG. 2. Distortion factor  $D_{L_{\max}}$  as a function of  $L_{\max}$  for  $Z=92$ , incident electron kinetic energy  $T_1=100$  MeV, photon energy  $\omega=20$  MeV, and scattering angles  $40^\circ$ ,  $100^\circ$ , and  $145^\circ$ .

clearly tends toward a constant value. For this case, using either Eq. (38) or Eq. (40) where  $d_{L_{\max}}$  is taken to be the average over the last five individual values lead to the same distorted wave cross section.

In Figs. 3 and 4 we show  $d_L$  and  $D_L$  for the same electron angles, but for energy loss  $\omega=40$  MeV and obtain similar results as for  $\omega=20$  MeV. In Figs. 5 and 6 we give the results for  $\omega=60$  MeV. For this case the results are not so favorable, particularly for the scattering angle

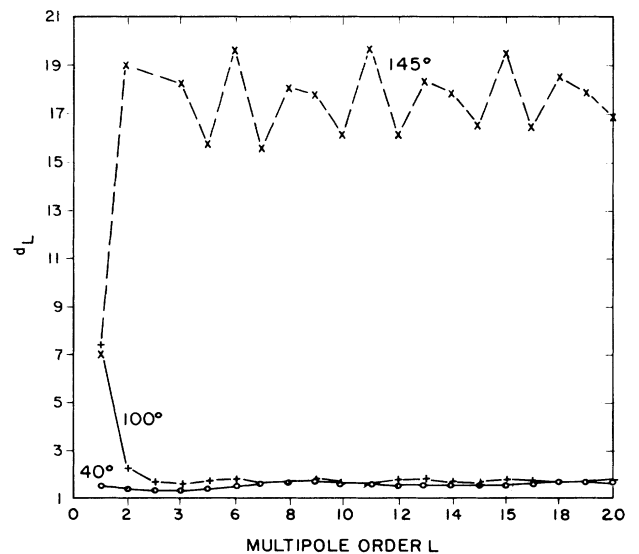


FIG. 3. Same as Fig. 1 except that the photon energy  $\omega=40$  MeV.

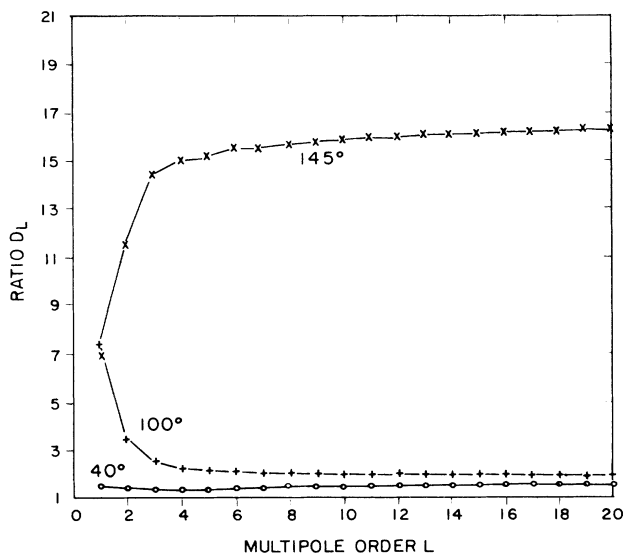


FIG. 4. Same as Fig. 2 except that the photon energy  $\omega=40$  MeV.

of  $40^\circ$ . As the energy of the photon emitted increases, the number of photon multipoles needed for the sum to converge increases. This behavior can be seen quite clearly for the plane wave case where we can calculate the individual multipole contributions and compare with the complete result. For  $\theta=40^\circ$ , for example, the percentage of the total plane wave sum for  $L_{\max}=20$  is 57% for  $\omega=20$  MeV, 55% for  $\omega=40$  MeV, and 49% for  $\omega=60$  MeV. The same percentages at  $145^\circ$  are 67%, 59%, and 53%. The more rapid convergence at larger scattering angles is a general result.

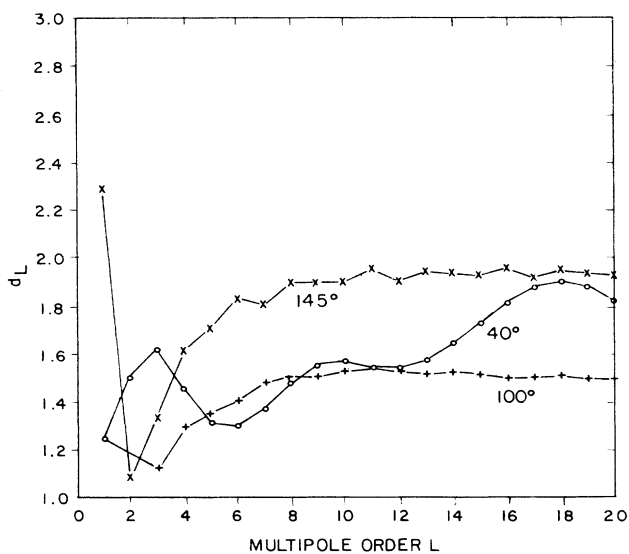


FIG. 5. Same as Fig. 1 except that the photon energy  $\omega=60$  MeV.

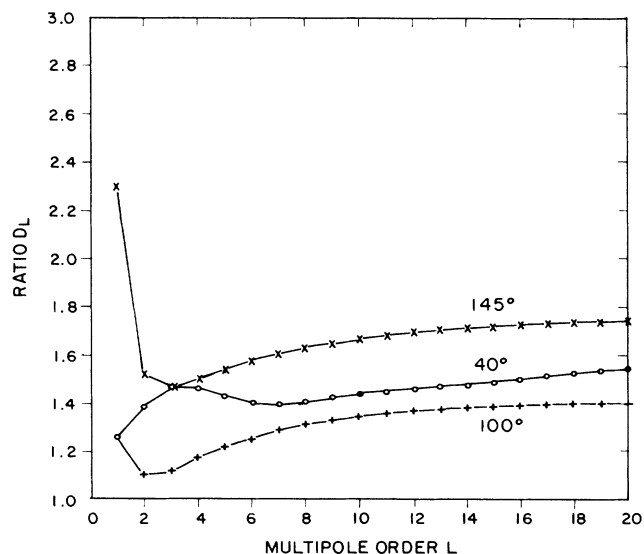


FIG. 6. Same as Fig. 2 except that the photon energy  $\omega=60$  MeV.

In Figs. 7 and 8 we show  $d_L$  and  $D_L$  for 50 MeV electrons emitting 35 MeV photons for forward scattering angles with multipole contributions up to  $L=30$ . As the scattering angle increases, the ratios  $d_L$  begin to oscillate about a constant value at smaller  $L$  values. The percentages of the plane wave result obtained by  $L=30$  for the angles  $30^\circ$ ,  $40^\circ$ ,  $50^\circ$ , and  $60^\circ$  are 65.7%, 67.7%, 68.9%, and

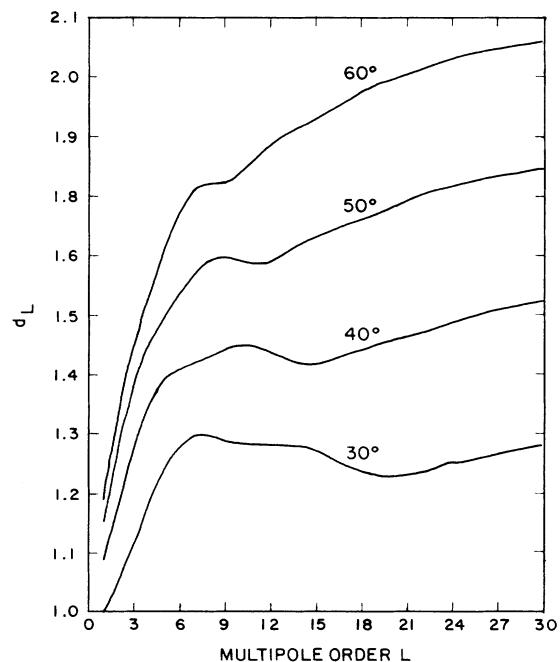


FIG. 7. Distortion factor  $d_L$  as a function of photon multipole  $L$  for  $Z=92$ , incident electron kinetic energy  $T_1=50$  MeV, photon energy  $\omega=35$  MeV, and scattering angles  $30^\circ$ ,  $40^\circ$ ,  $50^\circ$ , and  $60^\circ$ .

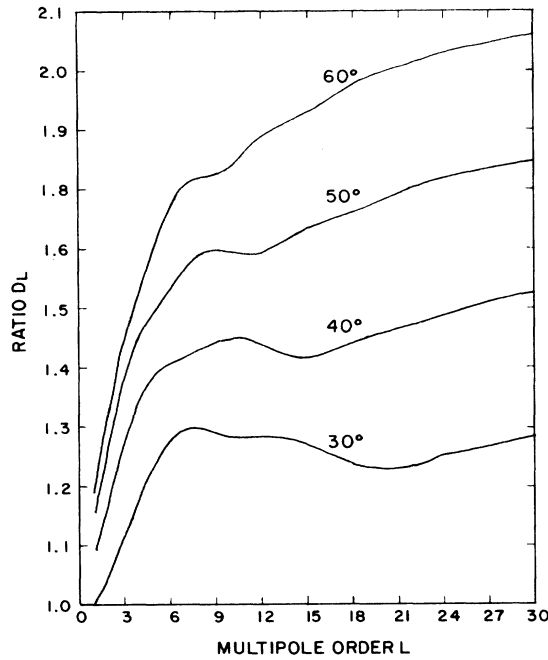


FIG. 8. Distortion factor  $D_{L_{\max}}$  as a function of  $L_{\max}$  for  $Z=92$ , incident electron kinetic energy  $T_1=50$  MeV, photon energy  $\omega=35$  MeV, and scattering angles  $30^\circ$ ,  $40^\circ$ ,  $50^\circ$ , and  $60^\circ$ .

69.7%. Upon examining these results we conclude that the most accurate value of the distorted wave cross section can be obtained by using an average value of  $d_L$  in Eq. (38) rather than trying to estimate the asymptotic value of  $D_L$  which in many cases is still changing. We typically average  $d_L$  over the last five values of  $L$  calculated. To get some estimate of the error made in such a procedure, we examine 10 MeV electron scattering from uranium at  $40^\circ$  losing 5 MeV. Since the energies are all lower, the angular momentum sums all converge more rapidly. In Table I below we give the average  $d_L$  value for different groups of multipoles, the percentage of the PW result accumulated by the maximum  $L$  value in the group, and the overall distortion factor  $D^{\text{DW}}$  arrived at by using the maximum  $L$  values in Eq. (38).

For this case, and a number of others we have examined, we find that if we calculate using  $\langle d_L \rangle$  in Eq. (38) and increasing  $L_{\max}$  until 60–70% of the PW sum is in-

TABLE I. Average values of  $d_L$ , percentage of the PW sum, and Coulomb distortion factor  $D^{\text{DW}}$  as a function of  $L$  for  $T_1=10$  MeV,  $\omega=5$  MeV,  $\theta=40^\circ$ , and  $Z=92$ .

$L$ 's	$\langle d_L \rangle$	% PW	$D^{\text{DW}}$
6–10	1.83	74	1.69
10–14	1.80	84	1.68
17–21	1.85	93	1.69
19–23	1.85	94	1.70

cluded in the sum, then the cross section we obtain is within 2% of the result obtained when the sum over 90% of the PW sum is included. In Fig. 9 we show the behavior of  $D_L$  as a function of  $L$  for this case.

#### IV. THE *AD HOC* PROCEDURE

In the plane wave approximation, bremsstrahlung is a second order process as shown in Figs. 10(a) and 10(b). Of the two vertices, one corresponds to an electron scattering elastically from the nucleus (essentially changing its direction) and the other corresponds to the emission of photon (with high probability of being emitted forward). Since the nuclear interaction is proportional to  $Ze^2$  while the photon emission is only proportional to  $e$ , the deviation from the plane wave result for medium and heavy nuclei is most likely due to the interaction at the nuclear vertex. This intuitive picture led to an *ad hoc* procedure for including Coulomb distortion in the plane wave formalism by modifying the nuclear charge form factor in Eq. (41). A distorted wave form factor is defined by writing

$$F_D^2(q) = \frac{\sigma_{\text{elastic}}(\theta_e, p)}{\sigma_{\text{Mott}}(\theta_e, p)}, \quad (45)$$

where  $\sigma_{\text{elastic}}$  is the elastic scattering differential cross section from the target nucleus for electrons with momentum  $p$  as a function of the scattering angle  $\theta_e$  calculated by phase shift analysis. The denominator is the Mott cross section for plane wave scattering from a point nucleus. The momentum transfer  $q$  and the scattering angle  $\theta_e$  are assumed to arise from the nuclear vertex. Therefore, the value of electron momentum  $p$  to be used in the distorted form factor is given by

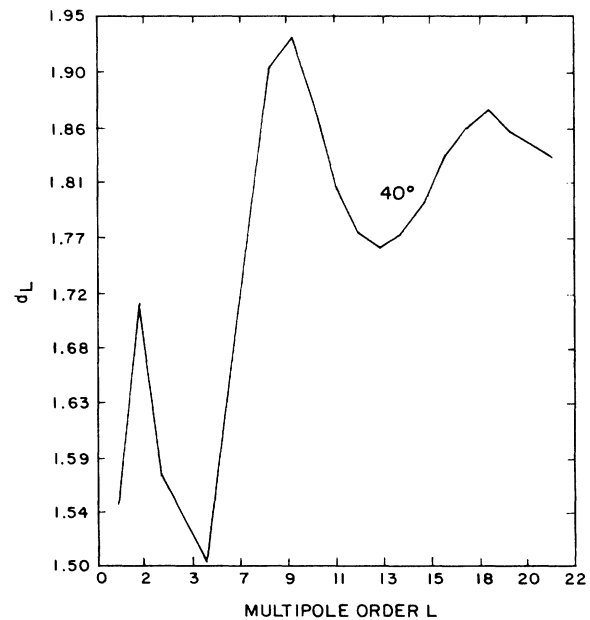


FIG. 9. Distortion factor  $d_L$  as a function of photon multipole  $L$  for  $Z=92$ , incident electron kinetic energy  $T_1=10$  MeV, photon energy  $\omega=5$  MeV, and scattering angle  $40^\circ$ .

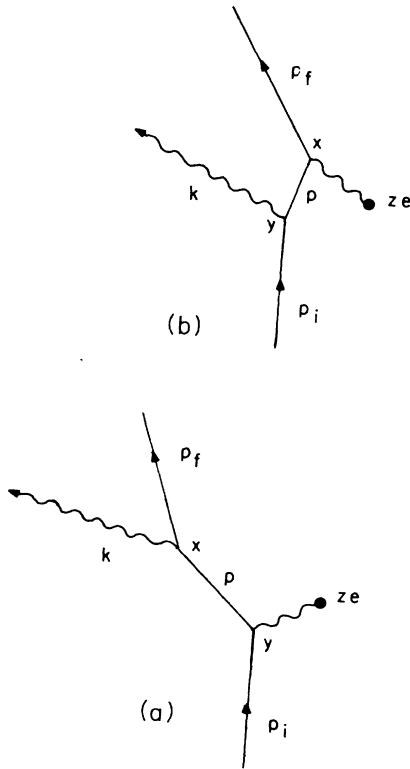


FIG. 10. Two possible Feynman diagrams for plane wave bremsstrahlung.

$$p = \frac{q}{2 \sin \frac{\theta_e}{2}} \quad (46)$$

When using the *ad hoc* procedure, the  $q$  integration in Eq. (41) is done numerically and for each value of  $q$  (and the observed electron scattering angle  $\theta_e$ ) a value of the electron momentum  $p$  is calculated. A phase shift program is run for  $p$  and  $\theta_e$  to calculate the distorted form factor which replaces the plane wave form factor in the integrand of Eq. (41). In practice, the elastic scattering program is run for a range of  $p$  values and the distorted form factors are stored in a large array and the value for any particular value of  $p$  is obtained by interpolation.

We have referred to this procedure by the term *ad hoc* since, apart from intuitively appealing considerations, we know of no good theoretical basis for the procedure. Bremsstrahlung has been calculated<sup>15</sup> by treating the radiation vertex to first order and the nuclear interaction to second order with plane waves. It was found that the ratio of the radiative cross section with the additional interaction at the nuclear vertex to the Bethe-Heitler result was approximately the same as the ratio of elastic scattering calculated with second order plane wave Born approximation to the first order plane wave Born approximation result. This result certainly is suggestive but including the second order plane wave Born approximation still furnishes a rather poor description of elastic electron scattering.

## V. RESULTS AND CONCLUSIONS

Since the DWBA calculation of the radiation tail is so time consuming, we decided to compare our results on a heavy nucleus (uranium) to the *ad hoc* procedure described in Sec. IV which has been used extensively by experimentalists. Any deviation between the DWBA results and the *ad hoc* procedure we find for uranium should be smaller for lighter nuclei.

In Fig. 11 we show the ratio  $[D^{\text{DW}}(\theta_e)]$  of the Coulomb distorted cross section [Eq. (38)] to the plane wave result [Eq. (41)] for the full DWBA and the same ratio  $[D^{\text{ad hoc}}(\theta_e)]$  using the *ad hoc* procedure instead of DWBA. One sees that the agreement between the two calculations is excellent, even within the diffraction minimum (or inflection) in the cross section around  $100^\circ$  where the distortion effects are quite large. We made such comparisons for a range of initial electron energies up to 160 MeV, energy losses and scattering angles. We find for low electron energies (either  $T_1$  or  $T_2$  less than 10–15 MeV) that the *ad hoc* procedure does not work very well. For lower electron energies the radiation is not so sharply peaked about the electron direction, and the assumption that almost all of the change in direction of the electron occurs at the nuclear vertex relies on the validity of the peaking approximation.

Apart from the low electron energies, we find that the agreement of the *ad hoc* procedure with our full DWBA result at a particular scattering angle depends only on the ratio of the energy loss to the incident electron energy  $\omega/T_1$ ; and for a given percentage of energy loss there is a weak dependence on electron scattering angle. To display

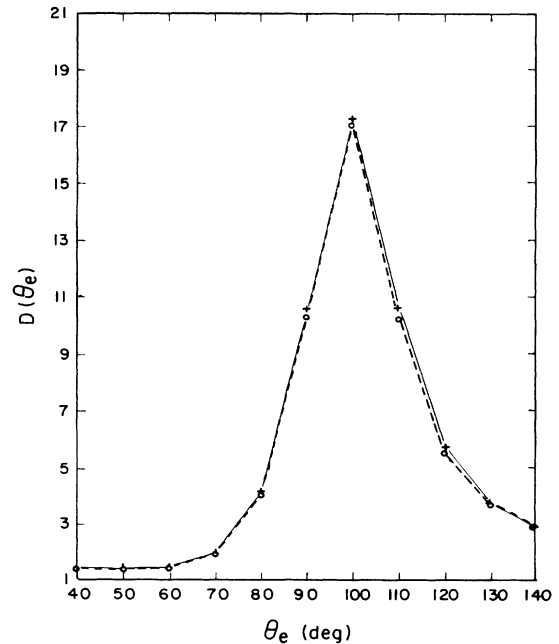


FIG. 11. Distortion factor  $D(\theta_e)$  as a function of scattering angle  $\theta_e$  for  $Z=92$ ,  $T_1=100$  MeV, and  $\omega=20$  MeV for the distorted wave (DW) and the *ad hoc* procedure shown by the solid and dashed lines, respectively.

TABLE II. Values of  $R = D^{DW} / D^{ad hoc}$  for  $Z = 92$  as a function of scattering angle  $\theta_e$  and percentage of energy loss with different values of  $L_{max}$  and  $T_1 \geq 50$  MeV.

$\omega/T_1$	$L_{max}$	30°	40°	50°	60°	70°	80°	90°	100°	110°	120°	130°	140°
20%	15	1.00	0.99	1.00	1.00	1.00	1.00	0.99	0.95	0.95	0.99	1.00	0.99
	20	0.99	1.00	0.99	1.00	1.00	1.00	0.98	0.99	0.97	0.97	1.01	1.04
30%	15	1.01	0.99	0.99	0.99	0.99	0.99	0.98	0.96	1.00	0.92	0.92	0.94
	20	0.99	1.00	0.99	0.99	0.99	0.99	0.98	1.00	0.95	0.95	0.91	0.94
40%	15	1.01	0.98	0.99	0.99	0.99	0.99	0.99	0.97	0.97	0.95	0.95	0.94
	20	0.97	0.99	0.98	0.99	0.99	0.99	0.98	0.98	0.96	0.96	0.95	0.94
60%	15	0.88	0.92	0.98	0.99	0.99	0.99	0.99	0.99	0.98	0.96	0.94	0.90
	20	0.94	1.00	0.97	0.98	0.98	0.98	0.99	0.98	0.98	0.96	0.93	0.90
70%	20	0.70	0.89	0.90	0.93	0.92	0.92	0.92	0.91	0.90	0.88	0.85	0.80
	25	0.91	0.92	0.94	0.93	0.92	0.92	0.92	0.91	0.90	0.88	0.85	0.80
	30	0.92	0.95	0.93	0.92	0.92	0.92	0.92	0.91	0.90	0.88	0.85	0.81

these results we calculate a ratio  $R$  of the Coulomb distortion factors for the DWBA analysis and for the *ad hoc* procedure. In Table II we show this ratio for a range of scattering angles and percentages of energy loss. Since for higher energy losses the convergence of the multipole sum in the DWBA analysis is somewhat uncertain, particularly for the smaller electron scattering angles, we show the number of multipoles included in the DWBA result for the case  $T_1 = 100$  MeV.

Upon examining the results of Table II, it is clear that the use of the *ad hoc* procedure for including the Coulomb distortion effects is, in general, very well justified. For energy losses less than 60% of the incident energy, the *ad hoc* distortion ratio is within 5% of the DWBA distortion ratio except for electron scattering angles larger than 120° even within diffraction minima. The 6% deviation at  $\theta_e = 30^\circ$  is probably due to incomplete convergence of the multipole sum in the DWBA result. The agreement for scattering angles between 40° and 100° for energy losses up to 40% is essentially perfect.

However, for larger energy losses and for larger scattering angles, the *ad hoc* procedure clearly overestimates the Coulomb distortion. For example, for  $\omega/T_1$  of 70% at  $\theta_e = 140^\circ$ , the *ad hoc* procedure overestimates the distortion by about 20%. At more forward scattering angles (40°–110°) this overestimate is less than 10%. Note that apart from 30° and 40°, the multipole sum for this case seems to have converged very well.

A direct measurement of the radiation tail from tungsten at  $\theta_e = 30^\circ$  with incident electron energies of 300 MeV was performed at Mainz by LeRose *et al.*<sup>8</sup> By measuring the radiation tail as a function of target thickness, they extracted the contribution arising from radiation in the field of the nucleus which we have calculated. The so-called internal bremsstrahlung tail was measured for energy losses up to about 70% of the incident energy, and apart from the lower energy loss regions where nuclear excitations were present, the experimental radiation tail agreed with the tail calculated with the *ad hoc* pro-

cedure quite well. We have not had enough computer time to repeat our entire calculation for tungsten at  $E_e = 300$  MeV but our table of results for uranium suggest that near the maximum energy loss measured in the experiment, deviations on the order of 8% should have begun to show up. However, at 30° our multipole sum has not completely converged for the larger energy losses so our predicted deviation of about 8% may be too large and the deviation for tungsten should be smaller than that for uranium. In any case, the errors quoted for the Mainz data are of order  $\pm 10\%$  in this energy loss region. Thus, our results are in complete agreement with the experimental data for energy losses up to 60%, and are not in disagreement at 70%. However, if such a measurement is made at  $\theta_e = 120^\circ$  or larger for 70% energy loss, we predict that the radiation tail calculated with the *ad hoc* procedure would rise about 12% above the experimentally extracted radiation tail.

In conclusion, we have successfully calculated the Coulomb distortion to the radiation tail accompanying elastic electron scattering. The variation in  $R$  with  $L_{max}$  shown in Table II is a rough measure of the uncertainty in our DWBA results. Apart from forward angles with large energy losses, our DWBA results are good to a few percent and the results given can be improved by using more computer time since we have not yet discovered any numerical difficulties with our calculational procedure. Upon comparing the DWBA results with an *ad hoc* procedure of including the Coulomb distortion effects in a plane wave formalism, we find that the *ad hoc* procedure works very well for energy losses less than 60% and reasonably well for energy losses up to 70%. We performed some calculations at energy losses of 80% of the incident electron energy and estimate that the *ad hoc* procedure overestimates the radiation tail by up to 25% at forward and backward angles, and by about 10–15% for mid-range angles. Apart from the large energy loss regions, the *ad hoc* procedure for evaluating the radiation tail accompanying elastic electron scattering can be used

with confidence that errors of only a few percent are being made. Even in the large energy loss region the errors are only on the order of 20% and the results given in Table II can be used to correct for this discrepancy.

This work was supported in part by DOE Grant No. DE-AC02-79ER10397-07.

## APPENDIX

### 1. Dirac-Coulomb radial integrals

To evaluate the radial integrals in Eqs. (21) and (22), we define the  $8 \times 4$  incomplete matrix gamma function

$$\Gamma(\mathcal{A} + 1, \mathcal{B}; R) = \int_R^\infty u_3(\omega r) \otimes u_2(p_2 r) \otimes u_1(p_1 r) dr, \quad (\text{A1})$$

where

$$u_3(\omega r) = \begin{bmatrix} j_L(\omega r) \\ j_{L-1}(\omega r) \end{bmatrix} \quad (\text{A2})$$

and

$$u_j(p_j r) = \begin{bmatrix} r g_{\kappa_j}^R(p_j r) & r g_{\kappa_j}^I(p_j r) \\ r f_{\kappa_j}^R(p_j r) & r f_{\kappa_j}^I(p_j r) \end{bmatrix}, \quad j = 1, 2. \quad (\text{A3})$$

For nonpenetrating orbits,  $\kappa_1$  and  $\kappa_2 > \kappa_{\text{mod}}$ , we take the limit  $R \rightarrow 0$ , and only require the first column of the gam-

ma matrix, to be denoted as  $\Gamma$ , which contains the regular Dirac-Coulomb functions.

The matrix array of functions  $u_j$ ,  $j = 1, 2$ , satisfies Eq. (26) with  $A$  and  $B$  matrices given in Eq. (27). The column vector of functions  $u_3$  also satisfies Eq. (26) with the matrices  $A_3 - 1$  and  $B_3$  given by Eq. (31). The  $8 \times 8$  matrices  $\mathcal{A}$  and  $\mathcal{B}$  are given in terms of the  $2 \times 2$   $A_i$  and  $B_i$ ,  $i = 1, 2, 3$ , by

$$\begin{aligned} \mathcal{A} &= A_3 \otimes I_4 + I_2 \otimes A_2 \otimes I_2 + I_4 \otimes A_1, \\ \mathcal{B} &= B_3 \otimes I_4 + I_2 \otimes B_2 \otimes I_2 + I_4 \otimes B_1, \end{aligned} \quad (\text{A4})$$

where  $I_n$  is the  $n \times n$  unit matrix.

All of these matrices can be transformed to either an  $A$ -diagonal or  $B$ -diagonal form. We can diagonalize the  $A$  matrices by using the transformation matrix

$$C^{SA} = \begin{bmatrix} (E\kappa - m\gamma)\sqrt{\kappa - \gamma} & p(\eta + i\gamma)\sqrt{\kappa + \gamma} \\ (E\kappa - m\gamma)\sqrt{\kappa + \gamma} & p(\eta + i\gamma)\sqrt{\kappa - \gamma} \end{bmatrix}. \quad (\text{A5})$$

The transformed  $A$  and  $B$  matrices are

$$A^{(A)} = \begin{bmatrix} \gamma & 0 \\ 0 & -\gamma \end{bmatrix}, \quad (\text{A6})$$

$$B^{(A)} = \frac{ip}{\gamma} \begin{bmatrix} -i\eta & \gamma - i\eta \\ \gamma + i\eta & i\eta \end{bmatrix}, \quad (\text{A7})$$

and the solution to Eq. (27) in the  $A$ -diagonal representation is

$$u^{(A)} = \begin{bmatrix} M_{-i\eta, \gamma - 1/2}(2ipr) & \frac{\gamma - i\eta}{2\gamma(2\gamma - 1)} M_{-i\eta, -\gamma + 1/2}(2ipr) \\ \frac{-(\gamma + i\eta)}{2\gamma(2\gamma + 1)} M_{-i\eta, \gamma + 1/2}(2ipr) & M_{-i\eta, -\gamma - 1/2}(2ipr) \end{bmatrix} \quad (\text{A8})$$

where  $M_{\kappa, \mu}(x)$  is the Whittaker function. The solution given in Eq. (28) in the standard representation can be obtained from  $u^{(A)}$  by the transformation

$$u^{(S)} = C^{SA} u^{(A)} N^{(S)}, \quad (\text{A9})$$

where the normalization constant  $N^{(S)}$  is a  $2 \times 2$  matrix given by

$$N^{(S)} = \begin{bmatrix} N(\gamma) & 0 \\ 0 & N(-\gamma) \end{bmatrix}, \quad (\text{A10})$$

where

$$N(\gamma) = e^{\eta\pi/2} e^{-i[\eta\kappa(\gamma) + \gamma\pi/2]} \frac{|\Gamma(\gamma + i\eta)|}{2p\sqrt{E + m} \Gamma(2\gamma + 1)(\gamma + i\eta)}. \quad (\text{A11})$$

The corresponding solutions for the spherical Bessel functions in  $A$ -diagonal form are

$$u_3^{(A)} = \begin{bmatrix} ij_{L-1}(\omega r) \\ j_L(\omega r) \end{bmatrix} \quad (\text{A12})$$

and the normalization constant and transformation matrix are

$$N_3 = \frac{(2i)^{-L-1} \omega^{-3/2}}{L(2L-1)!!} \quad (\text{A13})$$

and

$$C_3^{SA} = (2\omega^2 L^3)^{1/2} \begin{pmatrix} 0 & i \\ 1 & 0 \end{pmatrix}. \quad (\text{A14})$$

In a similar manner we can obtain a  $B$ -diagonal solution to Eq. (26) which is given by

$$u^{(B)} = \frac{1}{(2ipr)^{1/2}} \begin{pmatrix} M_{-1/2-i\eta,\gamma}(2ipr) & -\frac{(\gamma-i\eta)}{(\gamma+i\eta)} M_{-1/2-\eta,-\gamma}(2ipr) \\ M_{1/2-i\eta,\gamma}(2ipr) & M_{1/2-i\eta,-\gamma}(2ipr) \end{pmatrix} \quad (\text{A15})$$

and can be obtained from the  $A$ -diagonal solution by the transformation

$$C^{BA} = \begin{pmatrix} 1 & -\frac{(\gamma-i\eta)}{\gamma+i\eta} \\ 1 & 1 \end{pmatrix}. \quad (\text{A16})$$

The  $A$  and  $B$  matrices in  $B$ -diagonal form are given by

$$A^{(B)} = \begin{pmatrix} i\eta & \gamma-i\eta \\ \gamma+i\eta & -i\eta \end{pmatrix}, \quad B^{(B)} = \begin{pmatrix} -ip & 0 \\ 0 & ip \end{pmatrix}. \quad (\text{A17})$$

The Whittaker functions in Eq. (A15) can be expressed as a combination of Whittaker functions  $W_{k,\mu}$  of the second kind which leads to  $u_0^{(B)} = u_\infty^{(B)} T$  where

$$u_\infty^{(B)} = \frac{1}{(2ipr)^{1/2}} \begin{pmatrix} iW_{1/2+i\eta,\gamma}(-2ipr)e^{-\eta\pi} & -(\gamma-i\eta)W_{-1/2-i\eta,\gamma}(2ipr) \\ -i(\gamma+i\eta)W_{-1/2+i\eta,\gamma}(-2ipr)e^{-\eta\pi} & W_{1/2-i\eta,\gamma}(2ipr) \end{pmatrix} \quad (\text{A18})$$

and

$$T = \begin{pmatrix} \frac{\Gamma(2\gamma+1)}{\Gamma(\gamma+1+i\eta)} & -\frac{(\gamma-i\eta)}{\gamma+i\eta} \frac{\Gamma(-2\gamma+1)}{\Gamma(-\gamma+1+i\eta)} \\ \frac{e^{i\pi\gamma}e^{-\eta\pi}\Gamma(2\gamma+1)}{\Gamma(\gamma+1-i\eta)} & \frac{e^{-i\pi\gamma}e^{-\eta\pi}\Gamma(-2\gamma+1)}{\Gamma(-\gamma+1-i\eta)} \end{pmatrix}. \quad (\text{A19})$$

and  $u_\infty^{(B)}$  is also a solution to Eq. (26). The subscripts 0 and  $\infty$  denote power series and asymptotic series solutions, respectively.

For completeness we give the transformation from the  $B$ -diagonal solution to the standard representation by writing  $u^{(S)} = C^{SB}u^{(B)}N^{(S)}$  where  $N^{(S)}$  is given in Eq. (A11) and

$$C^{SB} = -(\gamma+i\eta) \begin{pmatrix} (\kappa-i\beta)\sqrt{E+m} & -(\gamma-i\eta)\sqrt{E+m} \\ i(\kappa-i\beta)\sqrt{E-m} & i(\gamma-i\eta)\sqrt{E-m} \end{pmatrix}, \quad (\text{A20})$$

where  $\beta = \alpha Zm/p$ .

Wright and Talwar<sup>5</sup> give a general method of evaluating integrals from 0 to infinity of products of Whittaker functions of these forms which permits the calculation of  $\Gamma$ . The electric and magnetic radial integrals of Eqs. (21) and (22) are given in terms of the elements of  $\Gamma$  in the standard representation by

$$I^{(m)} = \frac{\kappa_1 + \kappa_2}{[L(L+1)]^{1/2}} (\Gamma_2^{(S)} + \Gamma_3^{(S)}), \quad (\text{A21})$$

$$I^{(e)} = \left[ \frac{L}{L+1} \right]^{1/2} \left[ \Gamma_6^{(S)} - \Gamma_7^{(S)} + \Gamma_1^{(S)} + \Gamma_4^{(S)} + \frac{\kappa_1 - \kappa_2}{L} (\Gamma_6^{(S)} + \Gamma_7^{(S)}) \right], \quad (\text{A22})$$

where

$$\Gamma^{(S)} = C^{SB}S(\Delta_0, \Delta_0)C^{BA}\Gamma(\mathcal{A}^{(A)}+1, \mathcal{B}^{(A)}+\Delta_0) \times N_3N(\gamma_2)N(\gamma_1). \quad (\text{A23})$$

The various matrices  $C^{fi}$  in Eq. (A23) are  $8 \times 8$  matrices where  $i$  represents the initial representation and  $f$  the desired representation. They are formed from the corresponding  $2 \times 2$  matrices using Eq. (A4). The eight element vector gamma function in the  $A$ -diagonal representation represents the value of the radial integrals "off the mass shell" by the amount  $\Delta_0$ , and is given explicitly by the matrix series

$$\Gamma(\mathcal{A}^{(A)}+1, \mathcal{B}^{(A)}+\Delta_0) = \sum_{m=0}^{\infty} \frac{\Gamma(\mathcal{A}_{11}^{(A)}+m+1)\mathbf{V}_m}{\Delta_0^{\mathcal{A}_{11}^{(A)}+m+1}}, \quad (\text{A24})$$

where the vectors  $\mathbf{V}_m$  are defined by the initial value

$$(V_0)_i = \delta_{i,1}(2i\omega)^{L-1}(2ip_2)^{\gamma_2}(2ip_1)^{\gamma_1} \quad (\text{A25})$$

and the recursion relation

$$(\mathbf{V}_m)_i = \frac{\mathcal{B}_{ij}^{(A)}(\mathbf{V}_{m-1})_j}{\mathcal{A}_{11}^{(A)} - \mathcal{A}_{ii}^{(A)} + m}. \quad (\text{A26})$$

To achieve rapid convergence of the matrix series in Eq. (A24), the parameter  $\Delta_0$  is chosen to be  $7E_1$ . The  $8 \times 8$  matrix series  $S(\Delta_0, \Delta_0)$  operates on the radial integral off the mass shell and returns it to the physical value. While this can be done formally in one step, numerical difficulties require that this return to the physical value be done in a series of Zeno-like steps. That is, we write

$$S(\Delta_0, \Delta_0) = S(\delta, \delta)S(\Delta_0/2^n, \Delta_0/2^{n-1}) \cdots \times S(\Delta_0/4, \Delta_0/2)S(\Delta_0/2, \Delta_0), \quad (\text{A27})$$

where the last step has  $\delta = \Delta_0/2^n$  and returns the matrix of radial integrals to their physical argument. The individual  $S$  matrices are given by

$$S(x, \Delta) = \sum_{l=0}^{\infty} T_l x^l, \quad (\text{A28})$$

where  $T_0 = I_8$  and

$$T_l = (\mathcal{B}^{(B)} + \Delta)^{-1} \left[ \frac{\mathcal{A}^{(B)} + l}{l} \right] T_{l-1}.$$

Since the elements of  $\mathcal{B}^{(B)}$  are pure imaginary, for real  $x$  and  $\Delta$ , the series for  $S(x, \Delta)$  converges for all  $|x| \leq |\Delta|$  although the convergence may be quite slow. Choosing  $x = \Delta/2$ , the series for the various  $S$  matrices converge quite rapidly. In practice we perform between 15 and 20 Zeno-like steps before making the final step to the physical value. This procedure is necessary since two of the elements of the  $\mathcal{B}$  matrix are very small due to the extreme relativistic nature of the electrons in the bremsstrahlung process. The parameter  $\delta$  in the last step has become comparable to the size of these elements, and thus the series for the last  $S$  matrix also converges quite rapidly.

The matrix gamma function  $\Gamma(\mathcal{A} + 1, \mathcal{B})$  for  $R \rightarrow 0$  in Eq. (A1) has a useful recursion relation on the label  $L$  of the spherical Bessel function  $u_3^{(L)}(\omega r)$  defined in Eq. (A2). The recursion relations for the spherical Bessel function can be written as

$$u_3^{L \pm 1}(\omega r) = \left[ \frac{C_L^\pm}{r} - D_L^\pm \right] u_3^L(\omega r), \quad (\text{A29})$$

where

$$C_L^+ = \begin{bmatrix} \frac{2L+1}{\omega} & 0 \\ 0 & 0 \end{bmatrix},$$

$$C_L^- = \begin{bmatrix} 0 & 0 \\ 0 & \frac{2L-1}{\omega} \end{bmatrix},$$

$$D_L^\pm = \begin{bmatrix} 0 & \pm 1 \\ \mp 1 & 0 \end{bmatrix}.$$

Substituting this relation in Eq. (A1) (with  $R=0$ ) and using the general recursion relation for the matrix gamma function<sup>12,13</sup>  $\mathcal{A} \Gamma(\mathcal{A}, \mathcal{B}) = \mathcal{B} \Gamma(\mathcal{A} + 1, \mathcal{B})$ , one immediately obtains<sup>10</sup>

$$\Gamma(\mathcal{A}(L \pm 1) + 1, \mathcal{B}) = [(C_L^\pm \otimes I_4) \mathcal{A}(L)^{-1} \mathcal{B} - (D_L^\pm \otimes I_4)] \Gamma(\mathcal{A}(L) + 1, \mathcal{B}), \quad (\text{A30})$$

where the  $\mathcal{A}$  matrix dependence on  $L$  arises from  $A_3 - 1$  as shown in Eq. (A4).

For the case of penetrating orbits when either  $\kappa_1$  or  $\kappa_2 < \kappa_{\text{mod}}$ , the integrals from 0 to  $R$  are performed numerically and the integral from  $R$  to infinity is performed by using asymptotic expansions of the Whittaker functions. It is convenient to reduce the size of the matrices involved

by expanding the spherical Hankel function

$$h_L^{(1)} = \sum_{m=1}^{L+1} a_m(L) e^{i\omega r} / r^m, \quad (\text{A31})$$

where

$$a_m(L) = \frac{2\Gamma(L+m)i^{m-L+2}}{\Gamma(m)\Gamma(2+L-m)(2\omega)^m}$$

and defining a  $4 \times 4$  incomplete matrix gamma function

$$\Gamma(\mathcal{A} + 1 - m, (\mathcal{B} - i\omega); R) = \int_R^\infty \frac{e^{i\omega r}}{r^m} u_2 \times u_1 dr, \quad (\text{A32})$$

where

$$\mathcal{A} = A_2 \otimes I_2 + I_2 \otimes A_1, \quad (\text{A33})$$

$$\mathcal{B} = B_2 \otimes I_2 + I_2 \otimes B_1.$$

It is convenient to work in the  $B$ -diagonal representation of the Dirac-Coulomb functions so that the asymptotic expansions can be used. If we choose

$$u_3 = \begin{bmatrix} h_L^{(1)}(\omega r) \\ h_{L-1}^{(1)}(\omega r) \end{bmatrix}$$

we find that the upper  $4 \times 4$  elements of Eq. (A1) are given by

$$\int_R^\infty h_L^{(1)}(\omega r) u_2^{(B)} \otimes u_1^{(B)} dr = \sum_{m=1}^{L+1} a_m(L) \Gamma_0(\mathcal{A}^{(B)} + 1 - m, (\mathcal{B}^{(B)} - i\omega); R) \quad (\text{A34})$$

and the lower  $4 \times 4$  elements are given by the same expression with  $L = L - 1$ . To evaluate these integrals from  $R$  to infinity in Eq. (A34), we use Onley's asymptotic matrix series<sup>12</sup> for  $u^{(B)}$  as discussed in Wright and Talwar<sup>5</sup> to obtain

$$\Gamma_0^{(B)} = \Gamma_\infty^{(B)} (T_2 \otimes T_1), \quad (\text{A35})$$

where

$$\Gamma_\infty(\mathcal{A}^{(B)} + 1, \mathcal{B}^{(B)}; R) = \sum_{n=0} D_n \Gamma(\mathcal{A}^{(B)} + 1 - n; \mathcal{B}^{(B)} R) \mathcal{B}^{-(\overline{\mathcal{A}} + 1 - n)}. \quad (\text{A36})$$

The  $D$  matrices are defined by  $D_0 = (2ip_2)^{\overline{A}_2^{(B)}} \otimes (2ip_1)^{\overline{A}_1^{(B)}}$ , and the recursion relation

$$\{D_n\}_{ij} = \frac{\{(\overline{\mathcal{A}} + n - 1)D_{n-1}\}_{ij} + (\mathcal{A}_{ii} - \mathcal{A}_{jj})\{D_{n-1}\}_{ij}}{\mathcal{B}_{ii} - \mathcal{B}_{jj}}, \quad i \neq j$$

$$\{D_n\}_{ii} = -\frac{1}{n} \sum_{i \neq k} \mathcal{A}_{ik} \{D_n\}_{ki}, \quad (\text{A37})$$

where  $\overline{\mathcal{A}}$  is the diagonal part of the  $\mathcal{A}$  matrix and  $\underline{\mathcal{A}} = \mathcal{A} - \overline{\mathcal{A}}$ . The  $T$  matrices which transform the asymptotic series form of the gamma matrix to the power series form are given in Eq. (A19).

To extract the integrals over the spherical Bessel func-

$$\int_R^\infty j_L(\omega r) u_2^{(S)} u_1^{(S)} dr = \text{Re} \left[ N^{(S)} C^{SB} \sum_{m=1}^{L+1} a_m(L) \Gamma_0(\mathcal{A}^{(B)} + 1 - m, \mathcal{B}^{(B)} - i\omega; R) P \right], \quad (\text{A38})$$

where  $P$  is a  $4 \times 1$  matrix given by

$$P = \begin{bmatrix} A_2 \\ B_2 \end{bmatrix} \otimes \begin{bmatrix} A_1 \\ B_1 \end{bmatrix},$$

where  $A_i$  and  $B_i$  are the coefficients defined in Eq. (33) for the initial and final electron waves. The  $4 \times 4$  matrix  $C^{SB}$  transforms the wave functions from the  $B$ -diagonal to the standard representation and is given by  $C^{SB} = C_2^{SB} \otimes C_1^{SB}$  where  $C_i^{SB}$  is given in Eq. (A20). Finally,  $N^{(S)} = N_2^{(S)} \otimes N_1^{(S)}$  where  $N_i^{(S)}$  is defined in Eq. (A10).

## 2. Multipole decomposition of the Bethe-Heitler formula

In the plane wave second order calculation of bremsstrahlung first analyzed by Bethe and Heitler, the electron is elastically scattered by the nuclear Coulomb field and then emits a photon while interacting with the radiation field plus the opposite time sequence [see Figs. 10(a) and 10(b)]. Each of these two interactions of the electron is mediated by one photon, and the electrons are represented by Dirac plane waves. Using the standard Feynman rules and the notation of Bjorken and Drell<sup>16</sup> the transition matrix elements for this second order process is given by

$$S_{fi} = C \bar{u}(p_f, S_f) (T_1 + T_2) u(p_i, S_i), \quad (\text{A39})$$

where the constant  $C$  contains the energy conserving delta function and is given by

$$C = ie^3 Z \delta(E_f + \omega - E_i) (m^2 / 2E_i E_f \omega V^3)^{1/2}. \quad (\text{A40})$$

The operators  $T_1$  and  $T_2$ , corresponding to the two different second order diagrams, between the initial and final electron spinors with four momenta  $p_i = (E_i, \mathbf{p}_i)$  and  $p_f = (E_f, \mathbf{p}_f)$  can be written in terms of an integral over the intermediate three momentum  $\mathbf{p}$  as

$$T_1 = \int \frac{\epsilon^*(\gamma_0 E_i - \boldsymbol{\gamma} \cdot \mathbf{p} + m) \gamma_0}{(\mathbf{p}_i^2 - \mathbf{p}^2) |\mathbf{p} - \mathbf{p}_i|^2} F(|\mathbf{p} - \mathbf{p}_i|) \times e^{i(\mathbf{p} - \mathbf{p}_f) \cdot \mathbf{r}} e^{-ik \cdot \mathbf{r}} d^3 r d^3 p, \quad (\text{A41})$$

$$T_2 = \int \frac{\gamma_0 (\gamma_0 E_f - \boldsymbol{\gamma} \cdot \mathbf{p} + m) \epsilon^* F(|\mathbf{p} - \mathbf{p}_f|)}{(\mathbf{p}_f^2 - \mathbf{p}^2) |\mathbf{p} - \mathbf{p}_f|^2} \times e^{i(-\mathbf{p} + \mathbf{p}_i) \cdot \mathbf{r}} e^{-ik \cdot \mathbf{r}} d^3 r d^3 p, \quad (\text{A42})$$

where  $\epsilon_\mu^* = (0, \hat{\epsilon}^*)$  is the photon polarization and  $F$  is the

tion of order  $L$ , we form the appropriate linear combination of regular and irregular solutions by multiplying the right hand side of Eq. (A34) by a matrix  $P$ , transform it to the standard representation, multiply by the normalization constant, and take the real part. That is,

nuclear charge form factor introduced at the nuclear vertex to take into account the finite size of the nucleus.

To obtain the multipole decomposition of the plane wave result, we expand the photon field in multipoles by writing

$$\hat{\epsilon}_\mu^* e^{-ik \cdot \mathbf{r}} = \sqrt{2\pi} \sum_{LM} (2L+1)^{1/2} i^{-L} (-1)^{M+1} D_{-M, \mu}^L(\hat{\mathbf{k}}) \times [\mathbf{A}_{LM}^{\text{TM}}(\mathbf{r}) + i\mu \mathbf{A}_{LM}^{\text{TE}}(\mathbf{r})], \quad (\text{A43})$$

where  $D_{-M, \mu}^L$  are the rotation matrices and  $\mathbf{A}^{\text{TM}}$  and  $\mathbf{A}^{\text{TE}}$  are the transverse magnetic (TM) and electric (TE) Hansen solutions as given by Greiner and Eisenberg.<sup>17</sup> The label  $\mu$  denotes different polarization states of the photon. If we also use the Rayleigh expansion

$$e^{i(\mathbf{k}' \cdot \mathbf{r})} = 4\pi \sum_{lm} i^l j_l(k'r) Y_l^{*m}(\hat{\mathbf{k}}') Y_l^m(\hat{\mathbf{r}}) \quad (\text{A44})$$

for  $\mathbf{k}' = \mathbf{p}_f - \mathbf{p}$  in  $T_1$  and  $\mathbf{k}' = \mathbf{p} - \mathbf{p}_i$  in  $T_2$ , we can perform the space integrals in Eqs. (A41) and (A42). For example, the TM contribution to  $S_{fi}$  for photon polarization  $\mu$  is given by

$$(S_{fi}^{\mu})^{\text{TM}} = C \sum_{L, M, \lambda} \bar{u}(p_f, S_f) [\mathbf{B}_{\lambda, \mu}^{LM}(\mathbf{F}_1 + \mathbf{F}_1^C) \gamma_0 + \gamma_0 (\mathbf{F}_2 + \mathbf{F}_2^C) \mathbf{B}_{\lambda, \mu}^{LM}] \times u(p_i, S_i), \quad (\text{A45})$$

where

$$\mathbf{B}_{\lambda, \mu}^{LM} = [8\pi^5 (2L+1)]^{1/2} (-1)^{L+M+1} D_{-M, \mu}^L(\hat{\mathbf{k}}) \hat{\xi}_\lambda \quad (\text{A46})$$

and  $\hat{\xi}_\lambda$  are the spherical basis vectors for  $\lambda = 0, \pm 1$ . The integrals over  $d^3 p$  are written as a scalar integral  $I_1^{LM\lambda} = C_{M-\lambda, \lambda, M}^{L1L} G_1^{LM\lambda}$  where

$$G_1^{L, M-\lambda} = \int \frac{F(|\mathbf{p} - \mathbf{p}_i|) Y_L^{M-\lambda}(\hat{\mathbf{k}}'_f) \delta(k - k'_f)}{(\mathbf{p}_i^2 - \mathbf{p}^2) |\mathbf{p} - \mathbf{p}_i|^2 k^2} d^3 p \quad (\text{A47})$$

with  $F^C = m I_1^{LM\lambda}$  and  $F_1^0 = E_i I_1^{LM\lambda}$  and as a vector integral  $\mathbf{F}_1^{LM\lambda} = C_{M-\lambda, \lambda, M}^{L1L} \mathbf{G}_1^{LM\lambda}$  where

$$\mathbf{G}_1^{L, M-\lambda} = \int \frac{\mathbf{p} F(\mathbf{p} - \mathbf{p}_i) Y_L^{M-\lambda}(\hat{\mathbf{k}}'_f) \delta(k - k'_f)}{(\mathbf{p}_i^2 - \mathbf{p}^2) |\mathbf{p} - \mathbf{p}_i|^2 k^2} d^3 p. \quad (\text{A48})$$

The integrals with the subscript 2 are obtained by interchanging the labels  $i$  and  $f$  for  $E_i$ ,  $\mathbf{p}_i$ , and  $\mathbf{k}'_f$ .

The integrals  $G_{1,M-\lambda}^{L,M-\lambda}$  and  $G_1^{L,M-\lambda}$  can most easily be evaluated by choosing the vector  $\mathbf{p}_i - \mathbf{p}_f$  to define the  $z$  axis and for  $\mathbf{p}_i$  and  $\mathbf{p}_f$  to lie in the  $x-z$  plane with polar angles  $\theta_i$  and  $\theta_f$ , respectively. It is convenient to take  $\mathbf{k}'_f$  as the integration variable rather than  $\mathbf{p}$ . The integration over  $dk'_f$  is straightforwardly done by using the delta function in Eqs. (A47) and (A48). The  $\phi$  integration can be performed analytically by use of contour integration while the remaining integration over  $\theta$  is done numerically.

In terms of the matrix element  $S_{fi}$ , the second differential cross section in electron solid angle  $d\Omega_e$  and photon energy  $d\omega$  for bremsstrahlung is given by

$$\frac{d^2\sigma}{d\Omega_e d\omega} = \frac{k^2 p_f E_i E_f V^3}{(2\pi)^6 p_i T} \int \frac{1}{2} \sum |S_{fi}|^2 d\Omega_k dE_f, \quad (\text{A49})$$

where  $d\Omega_k$  is the solid angle into which the photon emerges and the summation is over spin and polarization directions. Using the standard techniques and substituting the expression for  $S_{fi}$  from Eq. (A45) into (A49) and integrating over photon angles  $d\Omega_k$  we obtain the differential cross section for TM photons of multipolarity  $L$ ,

$$\begin{aligned} \left[ \frac{d^2\sigma}{d\Omega_e d\omega} \right]_L^{\text{TM}} \\ = \frac{Z^2 \alpha^3 m^2 k p_f}{(2\pi)^2 p_i} \sum_{S_i, S_f} \left| \sum_{\lambda} \bar{u}(p_f, S_f) \Gamma_{\lambda} u(p_i, S_i) \right|^2, \end{aligned} \quad (\text{A50})$$

where

$$\Gamma_{\lambda} = \xi_{\lambda} (F_1 + F_1^C) \gamma_0 + \gamma_0 (F_2 + F_2^C) \xi_{\lambda}. \quad (\text{A51})$$

The spin sums can be reduced to traces by introducing the energy projection operators and Eq. (A50) can be written

$$\begin{aligned} \left[ \frac{d^2\sigma}{d\Omega_e d\omega} \right]_L^{\text{TM}} \\ = \frac{Z^2 \alpha^3 k p_f}{p_i} \sum_{\lambda_1, \lambda_2} \text{Tr}[\Gamma_{\lambda_1} (\not{p}_i + m) \bar{\Gamma}_{\lambda_2} (\not{p}_f + m)], \end{aligned} \quad (\text{A52})$$

where

$$\bar{\Gamma} = \gamma^0 \Gamma^{\dagger} \gamma^0.$$

Similarly, the cross section for TE photons of multipolarity  $L$  can be obtained with the integrals  $I_1^{LM\lambda}$  and  $F_1^{LM\lambda}$  defined by

$$\begin{aligned} I_1^{LM\lambda} = C_{M-\lambda, \lambda M}^{L L L-1} \left[ \frac{L+1}{2L+1} \right]^{1/2} G_1^{L-1, M-\lambda} \\ + C_{M-\lambda, \lambda M}^{L L L+1} \left[ \frac{L}{2L+1} \right]^{1/2} G_1^{L+1, M-\lambda}, \end{aligned} \quad (\text{A53})$$

$$\begin{aligned} F_1^{LM\lambda} = C_{M-\lambda, \lambda M}^{L L L-1} \left[ \frac{L+1}{2L+1} \right]^{1/2} G_1^{L-1, M-\lambda} \\ + C_{M-\lambda, \lambda M}^{L L L+1} \left[ \frac{L}{2L+1} \right]^{1/2} G_1^{L+1, M-\lambda}, \end{aligned} \quad (\text{A54})$$

where  $G_1$  and  $\mathbf{G}_1$  are defined in Eqs. (A47) and (A48). Finally, the bremsstrahlung cross section in Eq. (A49) can be written as the multipole sum

$$\frac{d^2\sigma}{d\Omega_e d\omega} = \sum_L \left[ \left[ \frac{d^2\sigma}{d\Omega_e d\omega} \right]_L^{\text{TM}} + \left[ \frac{d^2\sigma}{d\Omega_e d\omega} \right]_L^{\text{TE}} \right]. \quad (\text{A55})$$

Further details may be found in Ref. 18.

\*Present address: Escuela de Fisica, Universidad de Costa Rica, San Jose, Costa Rica.

<sup>1</sup>H. Bethe and W. Heitler, Proc. R. Soc. London Ser. A **146**, 83 (1934); W. Heitler, *The Quantum Theory of Radiation* (Oxford University Press, London, 1954).

<sup>2</sup>L. C. Maximon and D. B. Isabelle, Phys. Rev. **133**, B1344 (1964).

<sup>3</sup>L. W. Mo and Y. S. Tsai, Rev. Mod. Phys. **41**, 205 (1969).

<sup>4</sup>Yung-Su Tsai, Stanford Linear Accelerator Center Report No. 848, 1971; in Lectures: NATO Advanced Institute on Electron Scattering and Nuclear Structure, Proceedings of the Nato Conference on Electron Scattering and Nuclear Structure, Cagliari, Italy, 1970 (unpublished).

<sup>5</sup>L. E. Wright and Indu Talwar, J. Phys. A **19**, 1567 (1986).

<sup>6</sup>Farid Zamani-Noor, Ph.D. dissertation, Ohio University, 1984.

<sup>7</sup>F. Zamani-Noor and D. S. Onley, Phys. Rev. C **33**, 1354 (1986).

<sup>8</sup>John LeRose, Peter D. Zimmerman, C. C. Blatchley, J. Friedrich, N. Voegler, and M. Pieroth, Phys. Rev. C **32**, 449

(1985).

<sup>9</sup>W. W. Gargaro, Ph.D. dissertation, Ohio University, 1970.

<sup>10</sup>D. W. Kosik, Ph.D. dissertation, Ohio University, 1980.

<sup>11</sup>C. W. Soto Vargas, D. S. Onley, and L. E. Wright, Nucl. Phys. **A288**, 45 (1977); L. E. Wright, D. S. Onley, and C. W. Soto Vargas, J. Phys. A **10**, L53 (1977).

<sup>12</sup>D. S. Onley, *Nuclear Structure Studies Using Electron Scattering and Photoreaction* (Tohoku University, Sendai, 1972).

<sup>13</sup>K. Sud, L. E. Wright, and D. S. Onley, J. Math. Phys. **17**, 2175 (1976).

<sup>14</sup>D. R. Yennie, D. G. Ravenhall, and R. N. Wilson, Phys. Rev. **95**, 500 (1954).

<sup>15</sup>E. Borie, Lett. Nuovo Cimento **1**, 106 (1971).

<sup>16</sup>J. D. Bjorken and S. D. Drell, *Relativistic Quantum Mechanics*, (McGraw-Hill, New York, 1964).

<sup>17</sup>J. M. Eisenberg and W. Greiner, *Excitation Mechanisms of the Nucleus* (North-Holland, Amsterdam, 1970), Vol. II.

<sup>18</sup>Indu Talwar, Ph.D. dissertation, Ohio University, 1986.